Multiple links connect central carbon metabolism to DNA replication initiation and elongation in Bacillus subtilis

Hamid Nouri, Anne-Francoise Monnier, Solveig Fossum-Raunehaug, Monika Maciąg-Dorszyńska, Armelle Cabin-Flaman, François Képès, Grzegorz Węgrzyn, Agnieszka Szalewska-Palasz, Vic Norris, Kirsten Skarstad, et al.

DNA Research, 2018, 25(6), 641–653
doi: 10.1093/dnares/dsy031
Advance Access Publication Date: 26 September 2018
Full Paper

Full Paper

Multiple links connect central carbon metabolism to DNA replication initiation and elongation in *Bacillus subtilis*

Hamid Nouri[1,2,†], Anne-Françoise Monnier[2,‡], Solveig Fossum-Raunehaug[3,§], Monika Maciąg-Dorszyńska[4,¶], Armelle Cabin-Flaman[5,‖], François Képès[1,|||], Grzegorz Węgrzyn[4], Agnieszka Szalewska-Pałasz[4,¶], Vic Norris[5,||||], Kirsten Skarstad[3,#], and Laurent Janniere [1,2,*,]**

[1]iSSB, Génopole, CNRS, UEVE, Université Paris-Saclay, Evry 91000 France, [2]MICALIS, INRA, Jouy en Josas 78350, France, [3]Department of Cell Biology, Oslo University Hospital, University of Oslo, 0424 Oslo, Norway, [4]Department of Molecular Biology, University of Gdansk, 80-308 Gdansk, Poland, and [5]Laboratoire MERCI, AMMIS, Faculté des Sciences, 76131 Mont-Saint-Aignan, France

[†]Present address: Laboratoire de Microbiologie Appliquée, Faculté des Sciences de La Nature et de la Vie, Université de Bejaia, 06000 Bejaia, Algeria.
[‡]Present address: Centre de Recherche des Cordeliers, Université Paris Diderot, Université Paris Descartes, UPMC Université Paris 06 Sorbonne Universités, Sorbonne Paris Cité, INSERM, 75000 Paris, France.
[§]Present address: The Norwegian University of Life Sciences, 1430 Ås, Norway.
[¶]Present address: Department of Bacterial Molecular Genetics, University of Gdansk, 80-308 Gdansk, Poland.
[‖]Present address: Groupe de Physique des Matériaux, Faculté des Sciences et Techniques, 76801 Saint Etienne du Rouvray, France.
[|||]Present address: SYNOVANCE, Genopole Campus 1, Genavenir 6, 5 rue Henri Desbruères, F-91030 Evry, France.
[||||]Present address: Laboratory of Microbiology Signals and Microenvironment, Department of Biology, University of Rouen, 76131 Mont Saint Aignan, France.
[#]Present address: Molecular Microbiology, Department of Microbiology, Oslo University Hospital, Box 4950, 0424 Oslo, Norway.
**Present address: Génomique Métabolique, Genoscope, Institut François Jacob, CEA, CNRS, Univ Evry, Univ Paris Saclay, 91057 Evry, France.

*To whom correspondence should be addressed. Tel. 33 1 69 47 53 92. Fax. 33 1 69 47 44 37.
Email: laurent.janniere@issb.genopole.fr

Edited by Dr. Naotake Ogasawara

Received 31 January 2018; Editorial decision 16 August 2018; Accepted 17 August 2018

Abstract

DNA replication is coupled to growth by an unknown mechanism. Here, we investigated this coupling by analyzing growth and replication in 15 mutants of central carbon metabolism (CCM) cultivated in three rich media. In about one-fourth of the condition tested, defects in replication resulting from changes in initiation or elongation were detected. This uncovered 11 CCM genes important for replication and showed that some of these genes have an effect in one, two or three media. Additional results presented here and elsewhere (Jannière, L., Canceill, D., Suski, C., *et al.* (2007), PLoS One, 2, e447.) showed that, in the LB medium, the

CCM genes important for DNA elongation (*gapA* and *ackA*) are genetically linked to the lagging strand polymerase DnaE while those important for initiation (*pgk* and *pykA*) are genetically linked to the replication enzymes DnaC (helicase), DnaG (primase) and DnaE. Our work thus shows that the coupling between growth and replication involves multiple, medium-dependent links between CCM and replication. They also suggest that changes in CCM may affect initiation by altering the functional recruitment of DnaC, DnaG and DnaE at the chromosomal origin, and may affect elongation by altering the activity of DnaE at the replication fork. The underlying mechanism is discussed.

Key words: cell cycle, DNA replication, metabolism, signalling, integrative biology

1. Introduction

DNA replication must be coordinated with the cell cycle and cell division to ensure that chromosomes are faithfully replicated once and only once per cell cycle. This is carried out by overlapping mechanisms that control the activity of replication origins and replication enzymes for initiating DNA strand opening and recruitment of the replication machinery at origins every cell cycle.[1–3]

It has been known for several decades that replication is also subject to a metabolic control. In steady-state bacteria, this control couples the rate of replication to the rate of growth afforded by nutrients by modulating the initiation frequency and/or the speed of replication forks.[4–7] The net result is a precise and reproducible timing of DNA synthesis in the cell cycle across a wide range of nutritional conditions. Intriguingly, this timing primarily depends on the energy and precursors extracted from nutrients rather than on the actual nature of the carbon and nitrogen sources, as *Escherichia coli* cells growing at the same rate in different media exhibit similar temporal replication patterns.[5] The temporal control of replication in the cell cycle defines two major periods: the C period, which corresponds to the time taken to replicate the chromosome, and the D period, which corresponds to the time between termination of DNA replication and cell septation. At the growth rates analysed in this study (1–3 doublings/h (db/h)), the C and D periods are rather constant in *E. coli*[5,7] while they substantially vary in *Bacillus subtilis*[8] (see below). In chemostat cultures of *Saccharomyces cerevisiae* and possibly higher eukaryotes, the metabolic control confines DNA synthesis to the reduction phase of a redox metabolic cycle that is repeated several times per cell cycle.[9–11]

Despite a long history of investigation, the exact nature of the determinants involved in the metabolic control of replication remains elusive. Equally elusive is the mechanism at play and the way it acts in concert with classical control functions of replication initiation. The long-standing hypothesis is that the metabolic control of replication depends on the concentration of the active form of the replication initiator (DnaA–ATP) or on restricting DNA polymerases activity by limiting precursor concentrations. However, these concepts have been recently challenged.[12–14] Moreover, several groups argue that this control is a multifactorial process, which varies with nutrient richness and may involve sensing the cell's metabolism and communicating it to the replication machinery.[15–18] One example of such signalling involves the guanosine tetra- and penta-phosphate [(p)ppGpp]. This nucleotide analogue signals the metabolic status of bacteria and accumulates under nutritional stresses to inhibit the initiation or elongation phase of replication[19–22] and to impair the activity of the DnaG primase, an enzyme that synthesizes the short RNA primers used by DNA polymerases to replicate genomes.[23,24] However, although the replication inhibitory activity of (p)ppGpp at high concentration is well established, its role in DNA synthesis at low concentration (that is in the absence of nutritional stress) is still in debate.[13,25]

Central carbon metabolism (CCM) extracts the precursors and energy needed for macromolecular synthesis and biomass production from nutrients. This breakdown process involves about 30 key reactions that are highly conserved across the phyla. CCM is fed at various positions by different metabolites and the metabolite entry point determines the polarity of the carbon flux travelling through it, either glycolytic or gluconeogenic. The CCM catabolic reactions are grouped in pathways of which glycolysis, gluconeogenesis, the pentose phosphate pathway and the tricarboxylic acid (TCA) cycle form the main routes for breaking down nutrients (see the schematic representation in Supplementary Fig. S1). By directly sensing the supply and the demand in biosynthetic reactions, CCM is in a strategic position for producing signals that cells may use for adapting the main cellular activities to nutrient richness as recently demonstrated for cell division in *E. coli* and *B. subtilis*.[26–28]

A role for CCM in replication was first suggested in the model organisms *B. subtilis*, *E. coli* and *S. cerevisiae* by a series of related genetic studies that analysed the viability of thermosensitive replication mutants at high temperature in cells compromised in CCM genes. In *B. subtilis*, this analysis uncovered strong genetic links between the 3-carbon part of the glycolysis/gluconeogenesis pathway (i.e. *gapA*, *pgk*, *pgm*, *eno* and *pykA* see Supplementary Fig. S1) and three replication enzymes, namely the DnaC helicase, DnaG primase and DnaE polymerase.[29] Significantly, these three replication enzymes are loaded early at *oriC* during the initiation of replication and form a ternary complex in the replisome to carry out DNA melting and lagging strand synthesis.[30,31] This would make these enzymes good target candidates for modulating replication initiation and elongation in response to changes in CCM activity. In *E. coli*, studies have uncovered strong genetic links between *pta*, *ackA* and genes encoding pyruvate dehydrogenase subunits (*lpdA* and *aceE*) (Supplementary Fig. S1) and the replication initiator protein DnaA, linking CCM to initiation.[32–34] In the budding yeast, three glycolytic enzymes (HXK2, ENO2 and PGM1) were found genetically linked to MCM1[35] a multifunctional protein required for the stable maintenance of minichromosomes that binds DNA sequences to stimulate initiation of DNA synthesis and to regulate transcription of genes involved in diverse cellular functions including replication and the cell cycle.[36] Other, independent, studies further support the hypothesis of CCM-replication links. For instance, an alteration of replication initiation was detected in cells defective in the glycolytic enzymes GapA, PykA and PdhB in *B. subtilis*[13] and several CCM genes were found to be important for replication in eukaryotic cells.[37–40] The CCM-replication link may even be more complicated as a striking inter- and intra-cellular diversity in *E. coli* and *B. subtilis* metabolism was found[41] and we hypothesized that DNA replication may influence cell's metabolism.[42] To get insights into how CCM is linked to replication in *B. subtilis*, we analysed here the coupling between growth and replication in a library of 25 CCM mutants cultivated in three different rich media.

2. Materials and methods

2.1. Strains and plasmids

Strains and plasmids are listed in Supplementary Table S1. *B. subtilis* cells were grown at 37°C in LB supplement or not with malate 0.2% or in minimal medium (K_2HPO_4: 80 mM; KH_2PO_4: 44 mM; $(NH_4)_2SO_4$: 15 mM; $C_6H_5Na_3O_7$ $2H_20$: 3, 4 mM; $CaCL_2$: 50 mM; $MgSO_4$: 2 mM; FeIII citrate: 11 µg/mL; $MnCl_2$: 10 µM; $FeSO_4$: 1 µM; $FeCl_3$: 4 µg/mL; Trp 50 µg/mL) supplemented with glucose 0.4%, casein hydrolysate 0.2%, malate 0.4%, glutamine 0.4%, proline 0.4% and/or succinate 0.4%, as listed in Supplementary Table S2. Unless stated otherwise, antibiotics were used at the following concentrations: spectinomycin (Sp, 60 µg/mL); kanamycin (Km, 5 µg/mL); erythromycin (Em, 0.6 µg/mL); chloramphenicol (Cm, 5 µg/mL); phleomycin (Pm, 10 µg/mL). Liquid cultures were performed in a water bath under strong shaking (200–230 rpm). The LB medium is a complex rich medium that supports steady-state growth at $OD_{600\ nm}$ <0.3 and a gradual decrease of the growth rate up to saturation ($OD_{600\ nm}$ > 3).[43] The regimen is glycolytic in the first part of the growth curve as shown by direct measurement of the activity of promoters sensitive to the glycolytic (*gapA* promoter) and neoglucogenic (*pckA* and *gapB* promoters) carbon flux.[29]

The *E. coli* plasmid pMUTIN2-Pm is a derivative of pMUTIN2 (Em^R)[44] in which the *erm* gene was replaced by a Pm (*pmr)* marker. The plasmid pLJH88 and pLJH89 were constructed by replacing the small *Hind*III-*Nhe*I fragment of the *E. coli* plasmid pDR111 (Spc^R)[45] by PCR *Hind*III-*Nhe*I fragments produced from pALS10[46] and containing the *relAt* or *relAi* ORFs preceded by a ribosome-binding site, respectively. The *relA* constructions were then inserted at the *amyE* locus of the *B. subtilis* chromosome by double crossover event to permit RelAt and RelAi expression from the IPTG-dependent *Pspank* promoter. The plasmid pLJH90 is a Cm^R derivative of pLJH88. It was constructed by replacing the *spc*-containing *Hind*III-*Sac*II fragment of pLJH88 by the *cat*-containing *Hind*III-*Sac*II fragment of pDG1661.[47] The plasmids pLJH92 and pLJH93 are derivatives of pMTLBs72 which is a low (6) copy number, Cm^R *B. subtilis* plasmid.[48] They contain at the *Sma*I site a PCR fragment generated from pLJH88 or pLJH89 and containing the *relAt* or *relAi* gene under the control of *Pspank*. The pLJH160 plasmid is a pMUTIN2 (Em^R) derivative in which the small *EcoR*I-*BamH*I fragment was replaced by an *EcoR*I-*BamH*I PCR fragment containing the C-terminal region of *pykA* fused to a 12 bp long *linker* and the FLAG tag (5'*AGCGGTAGCGGT*GACTACAAAGACGATGACGACAAA3'). Upon insertion in the chromosome by single crossover, *B. subtilis* encodes a PykA protein tagged with FLAG. The plasmid pLJH162 is a pMUTIN2 (Em^R) derivative in which the small *EcoR*I-*BamH*I fragment was replaced by an *EcoR*I-*BamH*I PCR fragment containing the C-terminal region of *gapB* fused to the 12 bp long linker and the FLAG tag. The *gapB* region contains in addition a point mutation that inactivates the catalytic site of GapB (151SCT>AAA; TCATGCACC>GCGGCTGCA). The insertion of the plasmid in the *B. subtilis* chromosome by single crossover results in the production in an inactive, FLAG-tagged GapB protein. Plasmids pLJH198 and pLJH199 are derivatives of the *E. coli* pJL87 (Cm^R)[49] that harbours between the *Hind*III-*Nhe*I restriction sites, a PCR fragment containing the 5' end of *gapB* or *pckA*, respectively. Once inserted in the *B. subtilis* chromosome by single-crossover, the *gapB* or *pckA* gene are expressed from *Phyper-spank*, an IPTG-dependent promoter. The pLJH200 plasmid is a pDR111 (Spc^R) derivative[45] in which a *Hind*III-*Nhe*I PCR fragment containing the *B. subtilis pgk* ORF and its ribosome binding site was inserted between the corresponding restriction sites of the recipient plasmid. This plasmid allows insertion of the *pgk* gene at the *amyE* locus by double crossover and the inserted gene is expressed from the IPTG-dependent *Pspank* promoter. The plasmid pLH206 is a pLJH200 derivative in which the *spc* marker was replaced by a *cat* gene. This was done by inserting between the *Lgu*I-*Eco*RI restriction sites of pLJH200 a *Lgu*I-*Eco*RI PCR fragment containing the *cat* marker of pMTLBs72.[48] Plasmid constructions were carried out using the In-Fusion® HD Cloning kit (Clontech, France) and Stellar *E. coli* competent cells (Clontech, Saint-Germain-en-Laye, France). Constructions were checked by DNA sequencing. *B. subtilis* strains were constructed by transforming competent cells with genomic or plasmid DNA as indicated in Supplementary Table S1. The genotype of the transformants was controlled by PCR, phenotypes analysis and/or DNA sequencing.

2.2. Quantitative PCR

2.2.1. Measurement of the *ori/ter* ratio

Wild-type cells cured of prophages (TF8A) and containing or not CCM mutations were grown overnight in different liquid media in triplicates (with a very few exceptions, the three independent cultures were inoculated with different constructs). Saturated cultures were then diluted 500-fold in the same media and growth was carefully monitored using spectrophotometry. Samples for qPCR analysis were collected at low cell concentration ($OD_{600\ nm}$ 0.1–0.15) to ensure that cell cycle parameters are determined in steady-state cells and are not affected by the approach to the stationary phase or by changes in medium composition. The genomic DNA was extracted using a standard procedure[29] and every qPCR reaction was carried out using two technical repeats of 4–5 serial dilutions. A non-replicating control DNA (stage II sporlets[50]) was analysed simultaneously to the samples in about 1/3 of the qPCR plates. Primers for the marker frequency analysis (see Supplementary Table S3 for details) were used at 200 nM in 12 µl of the 1× SYBR qPCR Premix Ex Taq (Tli RNaseH Plus) (Ozyme, St Quentin en Yvelines, France) and DNA amplification was carried out as follows: denaturation: 95°C, 30s; amplification: (33 cycles) 95°C, 5 s and 60°C, 1 min. For every qPCR reaction, the primer efficiency (97 to 103%) was controlled. The *ori/ter* ratio of the non-replicating sporlets was 0.585 +/– 0.019, a value consistent with the size of the PCR products (Supplementary Table S3). The amplifications were carried out on a Mastercycler® ep *realplex* (Eppendorf, Le Pecq, Fr) and the ΔCq were determined automatically from the cycle threshold.

The *pgmIP* and *enoLP* metabolic mutants (DGRM353 and DGRM354, respectively) are thermosensitive (Supplementary Fig. S2). To determine the effect of these mutations on cell cycle parameters, the following procedure was followed. The strains were precultured over-night at 30°C in triplicates, diluted 1,000-fold for growth at restrictive temperature (47°C for *pgmIP* and 45°C for *enoLP*) and cell cycle parameters (growth, *ori/ter* ratio and the C period) were determined as above. Results (Supplementary Table S4) were then used to calculate the corresponding parameters at 37°C. For this, we first analysed the effect of temperature on growth, the *ori/ter* ratio and C period of the wild-type (TF8A), Δ*ytsJ* (DGRM350) and Δ*ytoI* (DGRM360) strains (these mutations are present in the *pgmIP* and *enoLP* strains, Supplementary Table S1). Results showed that temperature has nearly no effect on the *ori/ter* ratio while it changes the growth rate and the C period in a similar way in the three strains (Supplementary Fig. S3), as expected from previous studies.[13,51] They in addition showed that the Δ*ytsJ* and Δ*ytoI* mutations have no effect on the growth-*ori/ter* ratio coupling (compare data

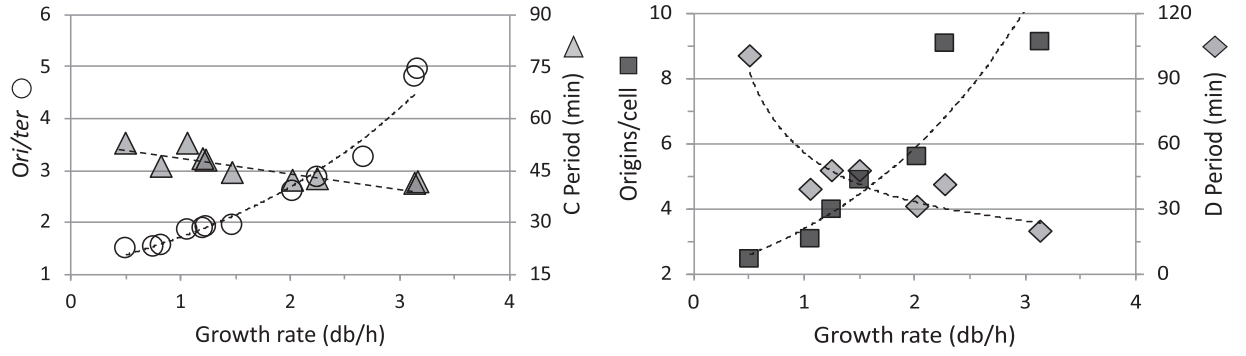

Figure 1. Growth-replication coupling in wild-type cells. Cell cycle parameters of wild-type cells (TF8A) growing exponentially for more than 10 generations in different media were determined: cell growth was monitored by spectrophotometry, the *ori/ter* ratio and C period by qPCR and the number of origins/cell as well as the D period by flow cytometry (see the text and Materials and Methods section for details). Left panel: *ori/ter* ratios and C periods plotted against growth rates. Right panel: numbers of origins/cell and D periods plotted against growth rates. The equations of the *ori/ter* ratio and C period curves (dotted lines) are: $y = 1.0942e^{0.4469x}$ and $y = -4.0435x + 52.835$, respectively. The *ori/ter* ratio and number of origins/cell are means of at least three independent replicates (SD/means <10%). The C periods were determined from representative experiments using 18 loci scattered on both arms of the chromosome and the D period was calculated from the number of origins/cell and the C period as indicated in the text.

Supplementary Fig. S3 37°C with Figs 1 and 2). The equation of the slopes Supplementary Fig. S3 were then used to derive the cell cycle parameters of the thermosensitive CCM mutants at 37°C (Supplementary Table S5).

2.2.2. Measurement of the C period

Cell growth, genomic DNAs extraction and amplification reactions were as above. Primer pairs, their positions on the chromosome map and the size of the PCR products are given Supplementary Table S3. Results were reported to the *ter*C signal and corrected for the size of the PCR products. The C period was extracted from the slope of the straight line of the plot $(\log_2 Nm)\tau$ against m where Nm is the relative copy number of a sequence N at position m (with $0 < m < 1$ along the *ori-ter* axis) and τ the generation time in minutes.[52] Control experiments showed that the marker frequency of the different loci in the non-replicating DNA was close to 1 (1.011 +/– 0.045) as expected. Similar data were obtained with primers on the right and left arm of the chromosome.

2.3. Flow cytometry analysis

2.3.1. Measurement of the number of origins/cell

Strains were grown as indicated in the previous section and at $OD_{600\ nm}$ 0.1–0.15, chloramphenicol (200 µg/mL final) was added to the cultures to impede replication initiation, cell division and allow completion of ongoing rounds of replication.[53] After 4–6 hours of drug treatment, 10^8 cells were fixed in filtered ethanol 70% and stored at 4°C. Stored cells were then washed in filtered 0.1 M of phosphate buffer (PB) pH 9, resuspended in 1 mL of Tris-buffered saline buffer (TBS 150, filtered) (20 mM Tris-HCl pH 7.5, 150 mM NaCl) and stained with Hoechst 33258 (1.5 µg/mL) for at least 30 min as described elsewhere.[51] Flow cytometry analysis was performed using a MoFlow Astrios cell sorter (Beckman Coulter, Life Sciences) equipped with a 355 nm krypton laser and a 448/59 nm bandpass filter used to collect Hoechst 33258 fluorescence. Data were analysed with the Kaluza software (Beckman Coulter, Life Sciences). We counted 50,000 to 100,000 events. In most of the tested samples, DNA histograms showed 1–2 main peaks with a 2^n distribution. The number of origins/cell was obtained from the proportion of cells with 1, 2, 4, 8 and/or 16 chromosomes.

2.3.2. Measurement of the D period

The D period was calculated from the equation $D = [(\ln(ori/cell)\tau/\ln(2)] - C$ where τ is the generation time and C the C period.[54]

2.4. Suppression assay

Three independently constructed mutants containing a *dna*(Ts) and the *ackA* deletion were grown overnight in LB at 30°C. Appropriate dilutions were then spread on solid LB medium and incubated at permissive (30°C) or restrictive temperature as indicated previously.[29]

2.5. Microscopy analysis

For analysing the production of filament in *dna*(ts) mutants, cells were grown overnight at 30°C in LB and diluted 500-fold in the same medium for further growth at permissive or restrictive temperature.[29] After 2 hours of incubation, cells were collected and the nucleoid was stained with 4',6'-diamidino-2-phenylindole (DAPI, 10 µg/mL) (Sigma). For analysing the effect of (p)ppGpp production on cell size, relevant strains were grown at 44°C in LB in the presence of different concentrations of IPTG. After about 10 generations of growth and at $OD_{650\ nm} = 0.4$, cells were collected and the membrane was stained by FM5-95 (Biotium Inc, Fremont, CA). Stained cells were then mounted on glass slides (VWR) covered with 1.2% agarose (low melting point, Sigma) in minimal medium supplemented with malate 0.2% and casa 0.2% and a 0.17 mm glass coverslip (VWR) was placed on top. The microscopy was performed on an epifluorescence microscope (Zeiss, Axio Observer.Z1) with a ×100 magnification oil-immersion objective (Plan-APOCHROMAT Ph3) and a CMOS camera (Orca Flash 4.0 LT Hamamatsu). Digital images were acquired and analysed using Zen 2012 software. All experiments were independently performed at least three times and representative pictures are shown.

2.6. (p)ppGpp analysis

The (p)ppGpp production in WT cells and (p)ppGpp mutants was analysed before and after induction of the stringent response by serine hydroxamate for *E. coli* and arginine hydroxamate (250 µM) for *B. subtilis*) as previously described.[55]

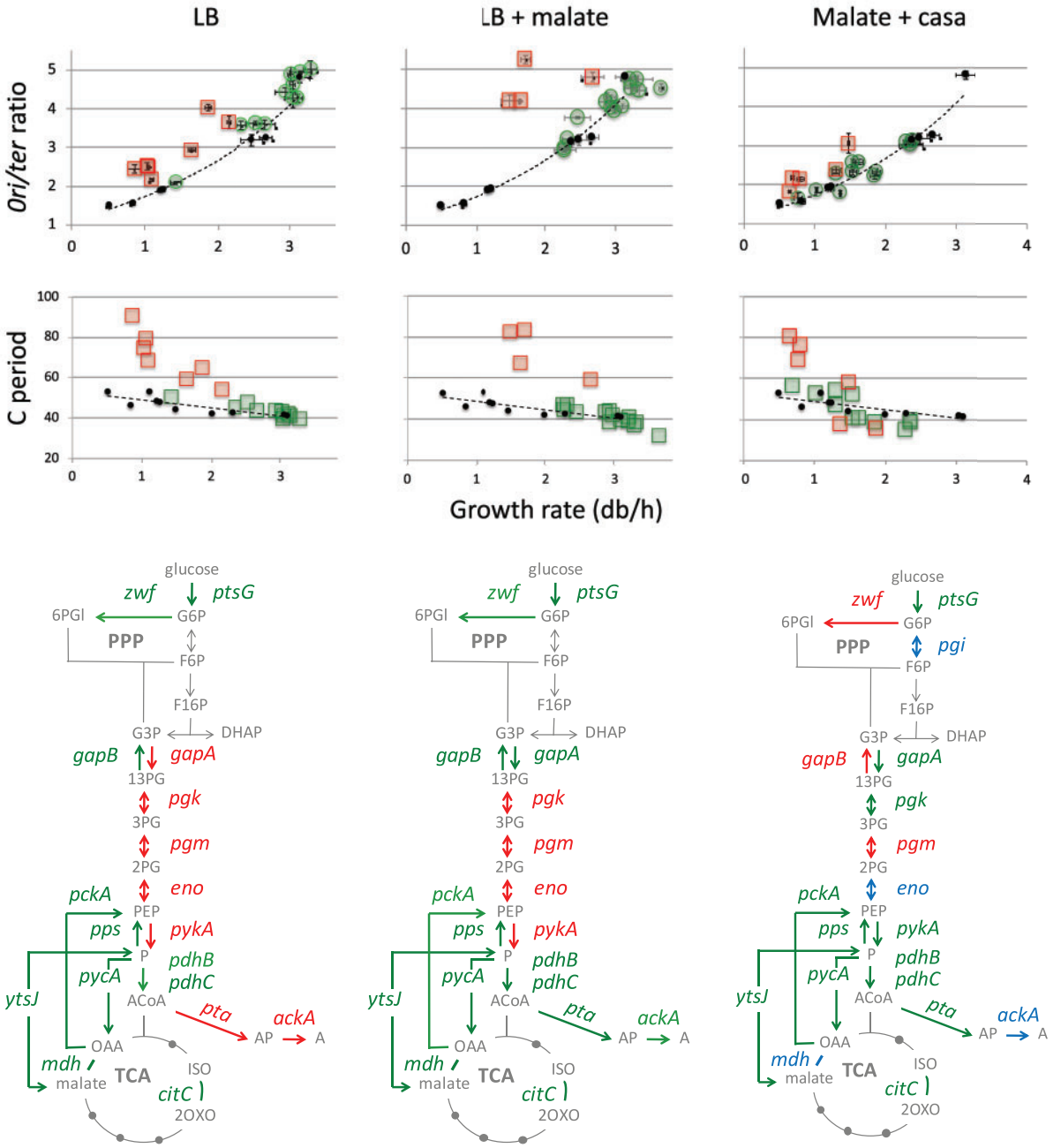

Figure 2. Identification of CCM mutations important for the growth-replication coupling in rich media. Top panels: Growth-*ori/ter* ratio and growth-C period coupling in CCM mutants grown in rich media (LB, LB + malate and malate + casa) (see Supplementary Table S5 for details). Closed dots and dotted line: results from wild-type cells (Fig. 1); Green and red symbols: CCM mutants with parameters that deviate from the typifying curve by less or more than 20%, respectively. Bars in the growth-*ori/ter* ratio relationship stand for mean and standard deviation obtained from at least three independent biological repeats (obtained generally from independent constructs) and two technical repeats (SD/mean < 10%). Bottom panels: Green symbols: CCM genes dispensable for both the growth-*ori/ter* ratio and growth-C period relationships (class I mutants). Red: CCM genes important for both relationships (class II mutants). Blue: CCM genes important for at least one relationship (class III mutants). *zwf*: glucose 6-phosphate dehydrogenase; *ptsG*: phosphoenolpyruvate: carbohydrate phosphotransferase enzymeIICBA; *pgi*: glucose 6-phosphate isomerase; *gapA*: glyceraldehyde-3-phosphate dehydrogenase, NAD-dependent; *gapB*: glyceraldehyde-3-phosphate dehydrogenase, NADP-dependent; pgk: phosphogycerate kinase; *pgm*: phosphoglycerate mutase; *eno*: enolase; *pykA*: pyruvate kinase; *pdhB*: pyruvate dehydrogenase (E1 beta subunit); *pdhC*: pyruvate dehydrogenase (dihydrolipoamide acetyltransferase E2 subunit); *pta:* phosphotransacetylase; *ackA:* acetate kinase; *citC*: isocitrate dehydrogenase; *mdh*: malate dehydrogenase; *ytsJ*: malic enzyme (NAPDH-producing); *pckA*: phosphoenolpyruvate carboxykinase; *pycA*: pyruvate carboxylase; *pps*: phosphoenolpyruvate synthase.

2.7. β-Galactosidase activity

The β-galactosidase activity encoded by the *bgaB* gene of *B. stearothermophilus* was measured as described previously.[56]

3. Results

3.1. Growth-replication coupling in wild-type cells

A hallmark of growing populations of *E. coli* and *B. subtilis* cells is the concurrent increase in the rate of growth and DNA synthesis.[5] This coupling implies that (i) bacteria growing slowly in poor carbon sources host a chromosome that either is not being replicated or is undergoing a single round of replication while (ii) fast-growing bacteria in rich media contain multi-forked chromosomes undergoing up to three overlapping replication cycles. To characterize in more detail the growth-replication relationship in *B. subtilis*, we quantified cell cycle parameters of a wild-type strain growing at rates ranging from 0.5 to 3 doublings per hour (db/h) in different media. This strain (TF8A) and the derivatives used below, are free of prophages to avoid any interference of phage induction on chromosomal replication.[57] Growth was assessed by spectrophotometry, and DNA replication by marker frequency using qPCR. In the latter analysis, the amount of replication terminus (*ter*) sequences was compared with the amount of 18 other loci regularly scattered along both arms of the chromosome and including the replication origin (*ori*). This gave us two major replication parameters: the relative copy number of *ori* versus *ter* sequences (the *ori/ter* ratio) and the C period. This latter parameter was extracted from the slope of the straight line of the plot $(\log_2 Nm)\tau$ against m where Nm is the relative copy number of a sequence N at position m (with $0 < m < 1$ along the *ori-ter* axis) and τ the generation time in minutes.[52] The results show a strong positive correlation between growth and the *ori/ter* ratio, as expected[5,6,13,51] (Fig. 1, left panel, Supplementary Table S2). They also show a significant negative correlation between growth and the C period: the time taken to replicate the chromosome increases from about 40 to 50 min when the growth rate decreases from 3 to 0.5 db/h. Calculation of the C period (C) from the *ori/ter* ratio and τ using the formula $ori/ter = 2^{C/\tau}$[58] confirms this negative correlation (Supplementary Table S2).

To get further insights into the growth-replication relationship, the number of origins/cell and the D period of the wild-type cells grown in various media were measured by flow cytometry. To that goal, we first analyzed the size of events detected by the flow cytometer in order to discriminate single cells from the chains of cells that often accumulate in fast growing *B. subtilis* cultures. This entailed using density plots of area versus width of fluorescence signals generated by cultures stained with a DNA specific dye (Hoechst 33258). Representative results are presented Supplementary Fig. S4 (left panels). The width axis corresponds to the flight time of particles through the laser beam spot. It reveals small (S) and large (L) events and that the proportion of large events strongly increases (from 1 to up to 60%) with the medium richness and growth rate. The area axis gives the integral of fluorescent signals. It shows that the intensity of fluorescence signals of small events varies while that of large events is rather constant and strong. Taken together, these results show that small events correspond to single cells while large events correspond to cell-chains and/or to clump of cells.

The samples used to measure the number of origins/cell and the D period corresponds to exponentially growing cultures treated for 4–5 hours with Cm. This treatment allows completion of ongoing replication cycles but prevents re-initiation of new rounds of replication and cell division.[53] Hence, at the end of the treatment, cells contain an integral number of fully replicated chromosomes that corresponds to the number of origins at the time of drug addition (replication run-out assay). It is of interest to note here that the proportion of cell-chains in Cm-treated cultures is greatly reduced (to 1–5%) as shown by density plots in Supplementary Fig. S4, right panels. DNA histograms of Cm-treated, single cells (Supplementary Fig. S5) show a smooth increase (from 2 to 6) of the number of origins/cell at growth rates ranging from 0.5 to 2 db/h followed by a stronger increase and a plateau to 9 origins/cell for cells growing at rates >2 db/h (Fig. 1, right panel and Supplementary Table S2). The D period, calculated from the equation $D = [(\ln(ori/cell)\tau/\ln(2)] - C$,[54] varies with the growth rate in *B. subtilis* as expected[8] (Fig. 1 and Supplementary Table S2).

Overall, the cell cycle parameters determined here show that the coupling between growth and replication in *B. subtilis* cells growing at rates >0.5 db/h depends on a concerted modulation of the initiation and elongation phases of replication. In agreement with *E. coli* studies,[5] they also support the hypothesis that this coupling depends on the precursors and energy extracted from nutrients rather than on the nature of available carbon sources.

3.2. Identification of CCM genes important for the growth-replication coupling

To look for a possible involvement of CCM in the growth-replication coupling, we analysed cell cycle parameters of CCM mutants grown in rich media and compared the results with data obtained for the wild-type strain grown in different carbon sources. We assumed that this approach is relevant as coupling depends on the energy and precursors extracted from nutrients and not on the amount and nature of nutrients available in the environment (see above). This assumption is further supported here by a coupling analysis in *B. subtilis* cells extracting energy and precursors from a rich medium (LB) at different rates because of inhibition of ribosome production. Such an assay was developed in *E. coli* using cells expressing a truncated form of the *E. coli* (p)ppGpp synthetase RelA from an inducible promoter. This truncated protein (termed RelAt) synthesizes constitutively the inhibitor of ribosome synthesis (p)ppGpp without the need for metabolic stress and binding to idling ribosomes.[59,60] This genetic system was proved to modulate *E. coli* growth rate and cell size in LB in an inducer-dependent manner. To develop a similar approach in *B. subtilis*, the *E. coli relAt* gene was inserted in the *B. subtilis* chromosome and put under the control of an IPTG inducible promoter. A related strain expressing an inactive form of *E. coli* RelA (RelAi) was constructed as a control. As in *E. coli*, an inverse correlation between (p)ppGpp production, growth rate and cell size was found in *B. subtilis* (see Supplementary data and Supplementary Fig. S6). Measurement of the *ori/ter* ratio shows a wild-type coupling over the large range of growth rates generated by degrees of (p)ppGpp production in LB (Supplementary Fig. S7). Hence, *B. subtilis* sets the replication rate according to the growth rate determined by its metabolism and not by the richness of the growth medium. It is thus reasonable to compare data from wild-type cells grown in various media to data from CCM mutants grown in rich media. This underpins our hypothesis that CCM mutants growing at various rates in rich media will have a wild-type growth-replication relationship unless the metabolic mutation alters cell cycle parameters.

We used a library of 25 CCM mutants and three rich media to analyse the growth-replication coupling in 53 metabolic conditions.

The mutations correspond to deletions (16), point mutations (5) or inducible transcriptional fusions (4). They decrease or abolish the activity of 19 genes (i.e. two-thirds of the key CCM genes; see Supplementary Table S1 for details on the strain library) that map in glycolysis (*ptsG*, *pgi*, *gapA, pgk, pgm, eno and pykA*), gluconeogenesis (*pckA* and *gapB*), the pentose phosphate pathway (*zwf*), the TCA cycle (*citC* and *mdh*), the overflow pathway (*pta* and *ackA*) and in the pyruvate metabolism (*pdhB, pdhC, ytsJ, pycA* and *pps*) (see the CCM map Supplementary Fig. S1 for details). The rich media (LB; LB + malate and the minimal medium + malate + casa – casein hydrolysate) feed both the upper and lower parts of CCM and support growth of mutants at rates ranging from about 0.5 to 3.5 db/h (see Materials and Methods and Supplementary Table S5 for details) (note that the Δ*pdhB* and Δ*pdhC* strains did not grow in malate + casa and that the Δ*pgi* mutant was not analysed in LB and LB + malate as cells had abnormal shapes in these media – not shown).

The growth rate, *ori/ter* ratio and C period in the 53 metabolic conditions were measured and compared with curves typifying the growth-replication coupling in wild-type cells (Fig. 2, top panels and see Supplementary Table S5 for details). Based on the SD/mean of experiments (<10%), we assigned the metabolic conditions into one of three classes. The first class (class I) contains the majority of conditions (34/53) and the growth-replication coupling appeared to be wild-type as the *ori/ter* ratio and the C period deviate by less than 20% from the typical wild-type curves. The second class (14/53) (class II) contains the conditions associated with a significant alteration of the growth-replication coupling with both the *ori/ter* ratio and the C period deviating by 20–120% from the typical wild-type curves. The third class (5/53) (class III) contains conditions in which a mixed phenotype is observed: the metabolic mutants exhibit a defect in only one replication parameter (the *ori/ter* ratio or the C period). Flow cytometry analysis shows that metabolic conditions conferring a class II phenotype at 37°C are also often associated with an increase in the number of origins/cell but not with a major change in the D period (this is of importance as changes in the D period may affect the growth-replication coupling by altering the timing of replication initiation) (Supplementary Fig. S8) [note that (i) mutations—*pgmIP* and *enoLP*—conferring a class II phenotype at high temperature were not analysed and that (ii) this analysis was limited to conditions conferring a growth rate ≤2 db/h as the growth-origins/cell reference curve is inaccurate at higher growth rates (Fig. 1, right panel)].

Taken together, the results show that the alteration of the growth-replication coupling in CCM mutants cultivated in rich media mainly results from an early firing of replication initiation and/or from a decrease in the mean velocity of fork progression. Hence, CCM is important for DNA replication. As initiation and elongation defects perturb replication cycles, our results suggest that a balanced CCM activity is needed for a normal timing of DNA replication in the cell cycle. Significantly, we did not observe a consistent correlation between reduced growth and replication defect indicating that a mere alteration of CCM activity and cellular metabolism is not sufficient to alter replication (Fig. 2).

Eleven CCM genes appear to be important for replication in rich media (Fig. 2, bottom panels). These genes are located in the main routes of carbon source degradation: the 6- and 3-carbon part of glycolysis/gluconeogenesis, the pentose phosphate pathway and the overflow pathway. Interestingly, the sets of genes important for replication differ from one medium to another with some genes being involved in just one medium (*zwf*, *pgi*, *gapA*, *gapB*, *pta* and *mdh*), and others being involved in two (*pgk*, *pykA* and *ackA*) or in three (*eno* and *pgm*) media (Fig. 2, bottom panels). It can thus be inferred that CCM is connected to DNA replication through multiple links that are committed in replication in a medium manner.

3.3. CCM mutations affect the initiation or elongation phase of replication

To determine which replication step is defective in CCM mutants, we constructed a series of strains replicating their genome from a plasmid replicon rather than from the chromosomal origin *oriC*. The replicon used (termed *oriN* thereafter) originates from the low copy-number plasmid pLS32. It encodes an initiator protein RepN that binds the plasmid origin embedded in the *repN* gene to initiate replication.[61,62] In addition to RepN, initiation at *oriN* depends on the host-encoded factors DnaD, DnaB (two helicase loaders), DnaC (the helicase) and DnaN (the DNA polymerase clamp). It is however independent of the initiator DnaA and the *oriC* sequence.[63] Once assembled at *oriN*, the initiation proteins (RepN, DnaB, DnaC and DnaD) recruit the rest of the chromosomal replication machinery to carry out bidirectional replication. In the series of strains constructed here, the plasmid replicon was inserted 2 kb to the left of the chromosomal origin and normal initiation of chromosomal replication was inactivated by introducing three ochre mutations into the DnaA-encoding gene or by deleting *oriC* sequences.[63,64]

The plasmid replicon used responds poorly to differences in carbon sources[13] (see below). This means that if uncoupling between growth and replication in CCM mutants were to result from changes in initiation (i.e. the productive interaction of DnaA with *oriC*), cells replicating their genome from the plasmid replicon would not suffer from the metabolic mutation and would thus exhibit the coupling of *oriN*-dependent cells, wild-type for metabolic functions. In contrast, if uncoupling were to result from changes in DNA elongation (or in an initiation event downstream of the formation of an active DnaA/*oriC* complex), plasmid replicon-dependent cells would still suffer from the metabolic mutation and would thus not exhibit the coupling typical of the CCM$^+$, *oriN*-dependent cells (i.e. growth and replication would be uncoupled).

We first analysed the growth-*ori/ter* coupling in *dnaA*^{ochre} or Δ*oriC* cells (which replicate the chromosome from *oriN*) growing in different media. As a control, an isogenic strain containing *oriN* and a functional chromosomal origin (DnaA+ OriC+) was analysed. The results show that this control strain (which contains *oriN* but does not depend on it) had the strong, positive relationship between growth and the *ori/ter* ratio characteristic of *B. subtilis* (Supplementary Fig. S9, top Table and panel) whereas *oriN*-dependent cells had a much weaker positive relationship (Supplementary Fig. S9, bottom Table and panel). This weaker response is probably because the plasmid replicon (i) is relatively insensitive to differences in the richness of media and (ii) cannot support high growth rates since it is unable to provide the high frequency of DNA initiation events required in rich media.

To determine which replication step is defective in CCM mutants, the growth-*ori/ter* ratio coupling in *oriN*-dependent derivatives was analysed as above. This analysis was focused on class II metabolic conditions where both the *ori/ter* ratio and the C period are affected at 37°C (i.e. the class II metabolic conditions affecting replication at high temperature and involving the *pgmIP* and *enoLP* mutations were not tested here, as the replication activity of the *oriN* replicon at high temperature is not known). Out of the nine tested metabolic conditions, four give a coupling typical of *oriN*-dependent cells while five exhibit a perturbed *oriN*-type coupling (Fig. 3 and

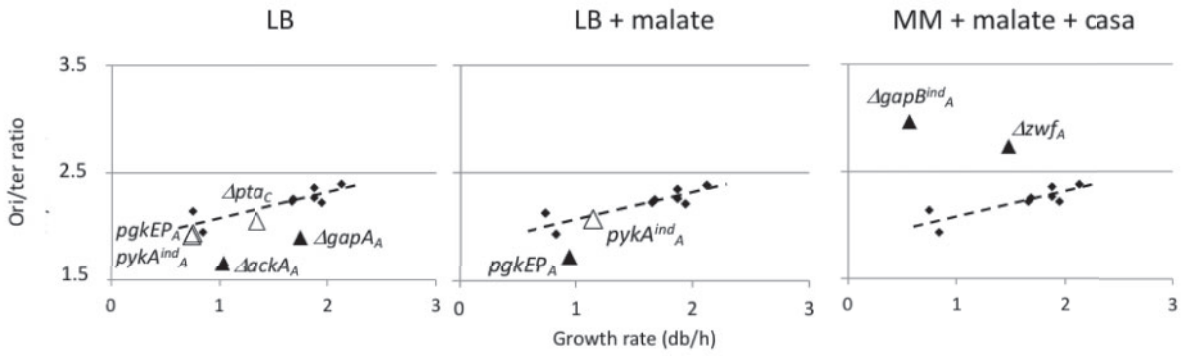

Media	Genotype (OriN$^+$ context)	Strain (DGRM)	Db/h	*ori/ter* ratio		Replication target
				data	Status	
LB	*dnaA* ^{ochre}	588	1.94	2.22	*oriN* -type	-
	ΔgapA dnaA ^{ochre}	596	1.75	1.90	Altered	Elongation
	pgkEP dnaA ^{ochre}	643	0.73	1.91	*oriN* -type	Initiation
	pykA ^{ind} *dnaA* ^{ochre}	584	0.74	1.93	*oriN* -type	Initiation
	Δpta ΔoriC	648	1.34	2.05	*oriN* -type	Initiation
	ΔackA dnaA ^{ochre}	641	1.03	1.66	Altered	Elongation
LB + malate	*pgkEP dnaA* ^{ochre}	643	0.95	1.73	Altered	Elongation
	pykA ^{ind} *dnaA* ^{ochre}	584	1.15	2.08	*oriN* -type	Initiation
MM + malate + casa	*dnaA* ^{ochre}	588	1.66	2.23	*oriN* -type	-
	Δzwf dnaA ^{ochre}	640	1.47	2.74	Altered	Elongation
	gapB ^{ind} *dnaA* ^{ochre}	585	0.56	2.97	Altered	Elongation

Figure 3. Identification of the replication step responding to CCM mutations. The growth and *ori/ter* ratio of CCM$^-$ *oriN*-dependent strains were determined in class II metabolic conditions and compared with the corresponding coupling curve of the CCM$^+$ *oriN*-dependent strain (Supplementary Fig. S9). Inserted table: Cell cycle parameters of the *oriN*-dependent CCM mutants grown in different media and replication target of CCM mutations (Initiation refers to the formation of an active DnaA/*oriC* complex and Elongation refers to a downstream initiation step or to the elongation phase of replication). Panels: Close diamonds and dotted lines: results from *oriN*-dependent, CCM$^+$ cells (Supplementary Fig. S9); Open triangles: CCM mutants with a relationship typical for *oriN*-dependent, CCM$^+$ cells; Close triangles: CCM mutants with a relationship different from the parental *oriN*-dependent, CCM$^+$ strain.

inserted table). As reasoned above, the loss of the uncoupling phenotype in *oriN*-dependent CCM mutants shows that the corresponding CCM mutations affect initiation (i.e. the formation of an active DnaA/*oriC* complex) at the chromosomal origin in *oriC*-dependent strains, while the persistence of this phenotype in *oriN*-dependent cells shows that the CCM mutations affect DNA elongation (or in a step downstream of the formation of an active DnaA/*oriC* complex) in the parental *oriC*-dependent strains. This interpretation is strengthened by control experiments showing that the assay is not sensitive to the way initiation at the chromosomal origin is abrogated (by the *dnaA*^{ochre} or Δ*oriC* mutation, Supplementary Fig. S10). Collectively, our results reveal that CCM genes are connected to the initiation (i.e. the formation of an active DnaA/*oriC* complex) or elongation (or an initiation step downstream of the formation of an active DnaA/*oriC* complex) phase of replication in a medium-dependent manner (Fig. 3). Although we investigated a limited number of class II conditions, links between CCM genes and different key replication phases were found in two out of the three tested media. This suggested that the mechanism of the growth-replication coupling in *B. subtilis*, which depends on a concerted modulation of the initiation frequency and elongation velocities (Fig. 1), may involve the combined effect of groups of CCM genes on the initiation and elongation phase of replication. This hypothesis is supported by the results presented below.

3.4. Genetic links between CCM and replication genes in LB

The cell cycle studies of *oriN*-dependent cells presented above show that the genes encoding catalysts of the terminal reactions of glycolysis (*gapA, pgk, pgm, eno* and *pykA*) and of downstream reactions (*pta* and *ackA*) are important for replication initiation (i.e. the formation of an active DnaA/*oriC* complex) or elongation (or a step downstream of the formation of an active DnaA/*oriC* complex) in the LB medium as summarized Fig. 4A, right part of the panel. Intriguingly, a previous study carried out in the same medium showed that *pgk, pgm, eno* and *pykA* are also genetically linked to the replication genes *dnaC*, *dnaG* and *dnaE*, while *gapA* is genetically linked to *dnaE*[29] (Fig. 4A, left part of the panel). Interestingly, the enzymes encoded by these replication genes (the helicase DnaC, the primase DnaG and the lagging strand polymerase DnaE) were recently shown to be required for the initiation and elongation phase of replication.[30,31,65–69] Indeed, during initiation of DNA replication, the conserved replication initiator DnaA protein, aided by the initiation factors DnaB, DnaD and DnaI (a helicase loader), melts the origin, *oriC*, to mediate anti-parallel loading of two hexameric rings of the DnaC helicase, one on each melted strand.[70] The primase, DnaG, and the lagging strand polymerase, DnaE, are then recruited to synthesize RNA primers and start DNA polymerization.[30,31] The remaining replisomal components, including the clamp, DnaN,

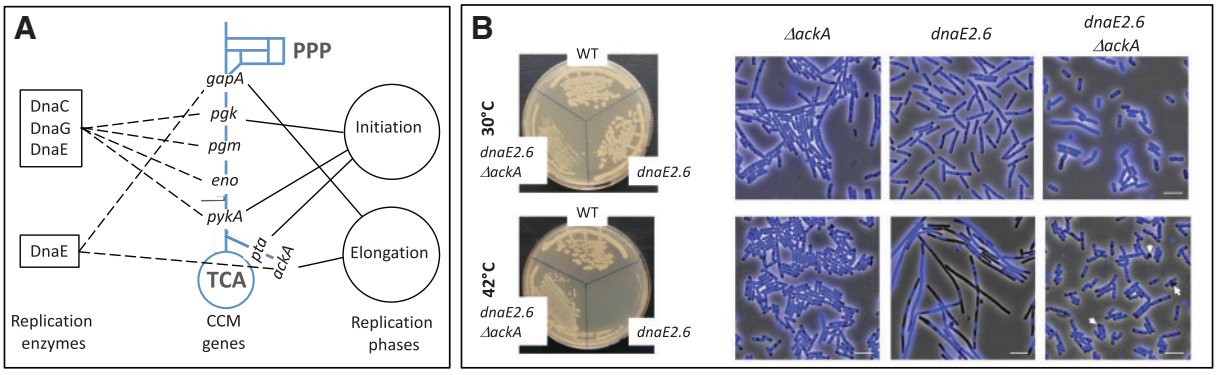

Figure 4. Suppression of *dnaE*(Ts) mutations in the Δ*ackA* context. (A): Functional (dark lines) and genetic (dotted lines) links between (i) CCM genes, (ii) the initiation and elongation phase of replication and (iii) the DnaC, DnaG and DnaE replication enzymes. (B): Viability and microscopy analysis of a Δ*ackA dnaE* (Ts) double mutant. Wild-type cells and strains carrying the thermosensitive *dnaE*2.6 mutations combined or not with the deletion of the *ackA* gene were grown in LB at permissive temperature. They were then streaked on LB plates or inoculated in liquid LB broth and then incubated at permissive or restrictive temperature. Left panels: colony formation at permissive (30°C) and restrictive (42°C) temperatures. Right panels: Microscopic analysis of cells grown at permissive or after 2 hours of incubation at restrictive temperature. Merge images of phase contrast and DAPI stained nucleoid (colored in blue). White arrows: anucleated minicells.

the clamp loader and the polymerase PolC, are then assembled to form two fully fledged replisomes with two different DNA polymerases (DnaE and PolC) that move away from *oriC* in opposite directions and replicate in a concerted manner the leading and lagging strands up to the terminus where the two replication forks merge.[68,69]

To extend to *ackA* our search for genetic links between CCM and replication genes in LB, we used the same method as previously (note that this method did not detect genetic links between *pta* and replication genes[29]). For this, we first constructed a series of Δ*ackA* strains containing a thermosensitive (Ts) mutation in replication genes. The double mutants were then tested for their viability (by plating) and ability to prevent filament formation (by microscopy) at restrictive temperature. Our results show that the *ackA* deletion restores viability and prevents filament formation at high temperature in every *dnaE*(ts) mutant tested (4/4) but failed to suppress thermosensitive mutations affecting other replication enzymes (namely: DnaB, DnaD, DnaC, DnaG, PolC, and DnaN) (Fig. 4B and Supplementary Table S6). Taken together, our results suggest that *pgk*, *pykA* (and possibly *pgm* and *eno*) are important for initiation (from the formation of the DnaA/*oriC* complex up to the recruitment of DnaC, DnaG and DnaE and the loading of two fully fledged replisomes) via an effect on DnaC, DnaG and DnaE while *gapA* and *ackA* are important for elongation via an effect on the lagging strand polymerase DnaE (Fig. 4A). This latter hypothesis is enforced by data showing that the deletion of *gapA* or *ackA* suppresses *dnaE*(ts) mutants mainly affected in DNA elongation.[31]

4. Discussion

We report here on a rather large study aimed at better understanding the important and likely universal relationship between central carbon metabolism (CCM) and DNA replication. To achieve this, we characterized the cell cycle parameters in three rich media of a collection of 25 CCM *B. subtilis* mutants. The results reveal defects in the initiation and/or elongation phase of replication in about one-third of the metabolic conditions tested. These defects are rather strong, causing a significant increase in the concentration of the origin sequences per cell and an up to 2-fold decrease in the mean velocity of replication forks. We infer from these results that CCM is important for replication and, in particular, for the coupling between growth and replication that positions the replication cycle within the cell cycle. These roles for CCM in replication are even more surprising as the replication phenotypes reported here were found in cells that are fully proficient in replication enzymes and replication control functions.

Overall, 11 genes mapping in different CCM pathways (the pentose–phosphate, glycolysis/neoglucogenesis, TCA and overflow pathways) appear to be important for replication in rich media (Fig. 2). Interestingly, their commitment in replication is medium dependent, forming partly overlapping subgroups with some genes only being needed for a single medium and others being needed for two or three media (Fig. 2). Moreover, some CCM genes are important for initiation while others are important for elongation or for both replication steps (*pgk*) (Fig. 3). Taken together, our results suggest that cells evolved a toolbox of intermingled CCM-replication links that it partially activates to cope with requirements imposed by the environment.

The results reported here show that the coupling between growth and replication in wild-type cells depends both on the modulation of the frequency of initiation and the mean velocity of replication forks (Fig. 1). Studies on CCM mutants confirm this conclusion (Figs 3 and 4) and suggest that this coupling may depend on both CCM-initiation and CCM-elongation links. It is thus tempting to speculate that these links are part of the metabolic control of DNA replication in *B. subtilis*.

Additional results presented here and in a previously publication uncover strong genetic links between six CCM genes (*gapA, pgk, pgm, eno, pykA* and *ackA*) and three replication genes (*dnaC*, *dnaG* and *dnaE*) in cells growing in the rich LB medium (Fig. 4A).[29] These links allow CCM mutations to restore the viability of thermosensitive replication mutants at restrictive temperatures. Interestingly, the links were suggested to depend on metabolic-induced conformational changes that restore the activity of the thermosensitive replication enzymes at restrictive temperature. They however may not dependent on a (i) deep change in the replication machinery that make thermosensitive replication enzymes dispensable for replication, (ii) the overexpression of *dna*(Ts) genes, (iii) a decay in the degradation of the thermosensitive replication protein, (iv) a reduction in ATP concentration or (v) an induction of a stress response.[29]

Moreover, the replication enzymes responding to CCM alteration encode the helicase DnaC, the primase DnaG and the lagging strand polymerase DnaE that are loaded early at *oriC* during the initiation of replication and form a ternary complex in the replisome for carrying out DNA melting, RNA priming and essential polymerase functions in lagging strand synthesis.[30,31] Although the suppression assay and the CCM-replication studies are based on distinct approaches and concepts, their combination gives us for the first time a coherent picture on how cell's metabolism and DNA replication may be coupled in LB. Indeed, results showed that at least two metabolic genes important for initiation (*pgk* and *pykA*) are genetically linked to *dnaC*, *dnaG* and *dnaE* while CCM genes important for elongation (*gapA* and *ackA*) are genetically linked to *dnaE* (Fig. 4). This suggests that, in the LB medium, CCM may modulate initiation by altering the functional recruitment of DnaC, DnaG and DnaE to *oriC* and may modulate DNA elongation by altering the activity of the polymerase DnaE in replication forks. This latter hypothesis is consistent with data showing that fork progression depends on lagging strand operations[71–74] and that the rate of DNA melting by helicases depends on the speed of DNA polymerases.[75–77] Along this line, the physical interaction between the helicase DnaC and the polymerase DnaE[30] may provide a direct means for adapting the rate of duplex unwinding and the concurrent synthesis of the leading and lagging strand to the activity of the DnaE polymerase.

How might CCM impact DNA replication? Long-standing hypotheses that the overall process of regulating replication depends on the concentration of the active form of the replication initiator (DnaA–ATP), on the sub-saturation of the replication machinery in precursors and/or on the concentration of (p)ppGpp have been challenged.[12–14] The results presented here also argue against the sub-saturation hypothesis, as there is no obvious correlation between the impact (positive or negative) of CCM mutations on replication precursor pathways (the main source of (d)NTPs and ATP are the pentose phosphate pathways and the TCA cycle, respectively) and their coupling or uncoupling phenotype (Fig. 2). Post-translational modification of replication enzymes is an alternative mechanism for the metabolism-replication coupling system as such modifications are important parts of the eukaryotic arsenal for regulating DNA replication.[78,79] Moreover, several lines of experimental evidence indicate that this level of regulation may also exist in bacteria. First, recent advances in proteomic technologies have uncovered post-translational modifications of numerous bacterial proteins including replication enzymes.[80–83] Second, independent studies show that the *E. coli* replication initiator DnaA is acetylated and its level of acetylation may play a critical role in regulating DNA replication initiation,[84] and that phosphorylation of the single-stranded DNA-binding (SSB) protein is important for replication in *B. subtilis*.[85,86] Third, indirect data suggest that the CCM-replication links detected in *B. subtilis* and *S. cerevisiae* depend on a metabolism-dependent allosteric regulation of replication enzymes.[29,35]

Post-translational modifications of replication enzymes are carried out by protein kinases/phosphatases and protein acetyltransferases/deacetylases in eukaryote cells. Such enzymes are thus potential effectors of the coupling between CCM and replication, although little is known on how their activity is regulated by metabolism (see however Ref. 87). An alternative way to achieve metabolism-dependent, allosteric-regulation of replication enzymes is via CCM itself. This group of catabolite reactions is central to the supply of precursors and energy from nutrients and to the demand in biosynthetic reactions, moreover, its activity responds almost immediately to changes in carbon sources. CCM is thus at a strategic position to dynamically integrate metabolism with replication. This dynamic integration may involve underexplored activities/functions of CCM metabolites and proteins. Indeed, several CCM metabolites have emerged as important modulators of various cellular activities by modulating dynamically protein activities via post-translational modifications or allosteric binding (see as reviews).[88,89] Key metabolites among others are acetyl-coenzyme A and ATP, which are the major donors of acetyl and phosphoryl groups, respectively, and acetyl phosphate which lies at the crossroads between protein phosphorylation and protein acetylation.[90–93] In addition, CCM enzymes from bacteria to eukarya are often multi-functional proteins carrying out both catalysis of a canonical metabolic reaction and non-metabolic functions involved in processes as diverse as DNA replication, transcription, cell division, signalling, apoptosis and pathogenicity. These moonlighting activities, found in the cytoplasm and the nucleus, involve novel enzymatic activities (like protein kinase activity) and/or interactions with non-metabolic enzymes (see for instance Refs. [94–97]). We are currently exploring the fascinating possibility that the CCM-replication links in *B. subtilis* involve moonlighting activities of CCM enzymes and/or signalling metabolites.

DNA double-stranded breaks are chromosomal lesions with a high mutagenic potential.[98,99] Their frequency increases in response to replication control defects and the importance of this threat is highlighted by the presence of multiple mechanisms ensuring faithful genome duplication once per cell cycle, and preventing re-initiation of replication.[100,101] In cells with aberrant timing of initiation, re-initiation of replication may increase the risk of double-stranded breaks by collision between forks or by forks encountering gaps in the DNA template. Such a risk may also increase in cells with a lengthened C period in consequence of a higher probability of fork breakage over time. Through their effect on replication and the timing of DNA synthesis in the cell cycle, the CCM-replication links described in this study may thus form a new determinant of genetic stability. In support of this hypothesis, it was found in *E. coli* that CCM mutations influence the fidelity of DNA replication[102] and that mutants of the *ackA-pta* overflow pathway, which is genetically connected to the replication initiator DnaA,[32,33] accumulate double strand breaks.[103] Moreover, mutants of the budding yeast impeded in the temporal control of DNA replication may exhibit substantial increases in the spontaneous mutation rate.[104] Further investigations are required to better evaluate the mechanism of CCM-replication links and its role in genetic stability and potentially in cancer as early events engaging normal human cells into the path in tumorigenesis involve major changes in CCM activity (the Warburg effect) and genetic instability.[105–107]

Acknowledgements

We thank S. Aymerich, R. Losick, D. Le Coq, Y. Tosawa, D. Jahn, E. Dervyn, M. Hecker, A. Grossman, S. Moriya and W. Haldenwang for strains and plasmids and Nathalie Vega-Czarny for assistance with the Moflow Astrio cell sorter. We are grateful to S. D. Ehrlich for his long interest in this work, and to S. Aymerich, I. Junier, O. Rivoire, B. Jester and P. Soultanas for helpful discussions and/or critically reading of the manuscript.

Conflict of interest

None declared.

Funding

This study was supported by the following grants: ROBUST (Génopole/Toulouse White Biotechnology (TWB)) to F.K.; SYNPATHIC (ANR) to F.K.;

UEVE (Université Evry Val d'Essonne; FRR2014 et FRR2017 Projet Recherche; FRR2016 Mobilité sortante) to L.J.; Norwegian Research Council to K.S.; the National Science Center (Poland, grants no. 2011/02/A/NZ1/00009 and UMO-2016/23/D/NZ1/02601 to G.W and M.M.-D., respectively). H.N. and A.-F.M. were supported by PhD fellowships from the MESR (Ministère de l'Enseignement Supérieur et de la Recherche; ED GGC, Université Paris Sud) and the Région Haute Normandie and INRA (ED NCB, Université de Rouen), respectively. L.J. and F.K. are on the CNRS staff. Funders had no role in study design or interpretation of results.

Supplementary data

Supplementary data are available at *DNARES* online.

References

1. Jameson, K. and Wilkinson, A.J. 2017, Control of initiation of DNA replication in *Bacillus subtilis* and *Escherichia coli*, *Genes*, **8**, 22–32.
2. Sclafani, R.A. and Holzen, T.M. 2007, Cell cycle regulation of DNA replication, *Annu. Rev. Genet.*, **41**, 237–80.
3. Skarstad, K. and Katayama, T. 2013, Regulating DNA replication in bacteria, *Cold Spring Harb. Perspect. Biol.*, **5**, a012922.
4. Skarstad, K., Boye, E. and Steen, H.B. 1986, Timing of initiation of chromosome replication in individual *Escherichia coli* cells, *Embo J.*, **5**, 1711.
5. Helmstetter, C.E. 1996, *Timing of synthetic activities in the cell cycle*. In: Neidhart, F.C., Curtis, R.I., Ingraham, E.C., Lin, K.B., and (null), L.E.C.C., (eds.), *Escherichia coli and Salmonella. Cellular and Molecular Biology*. Washington DC: ASM Press, pp. 1591–605.
6. Sharpe, M.E., Hauser, P.M., Sharpe, R.G. and Errington, J. 1998, *Bacillus subtilis* cell cycle as studied by fluorescence microscopy: constancy of cell length at initiation of DNA replication and evidence for active nucleoid partitioning, *J. Bact.*, **180**, 547–55.,
7. Michelsen, O., de Mattos, M.J.T., Jensen, P.R. and Hansen, F.G. 2003, Precise determinations of C and D periods by flow cytometry in *Escherichia coli* K-12 and B/r, *Microbiology (Reading, Engl.)*, **149**, 1001–10.
8. Holmes, M., Rickert, M. and Pierucci, O. 1980, Cell division cycle of *Bacillus subtilis*: evidence of variability in period D, *J. Bacteriol.*, **142**, 254–61.
9. Klevecz, R.R., Bolen, J., Forrest, G. and Murray, D.B. 2004, A genome-wide oscillation in transcription gates DNA replication and cell cycle, *Proc. Natl. Acad. Sci. USA.*, **101**, 1200–5.
10. Tu, B.P., Kudlicki, A., Rowicka, M. and McKnight, S.L. 2005, Logic of the yeast metabolic cycle: temporal compartmentalization of cellular processes, *Science*, **310**, 1152–8.
11. Burnetti, A.J., Aydin, M. and Buchler, N.E. 2016, Cell cycle Start is coupled to entry into the yeast metabolic cycle across diverse strains and growth rates, *Mboc.*, **27**, 64–74.
12. Mathews, C.K. 2015, Deoxyribonucleotide metabolism, mutagenesis and cancer, *Nat. Rev. Cancer* **15**, 528–39.
13. Murray, H. and Koh, A. 2014, Multiple regulatory systems coordinate DNA replication with cell growth in *Bacillus subtilis*, *PLoS Genet.*, **10**, e1004731.
14. Flåtten, I., Fossum-Raunehaug, S., Taipale, R., Martinsen, S. and Skarstad, K. 2015, The DnaA protein is not the limiting factor for initiation of replication in *Escherichia coli*, *PLoS Genet.*, **11**, e1005276.
15. Zyskind, J.W. and Smith, D.W. 1992, DNA replication, the bacterial cell cycle, and cell growth, *Cell*, **69**, 5–8.
16. Boye, E. and Nordström, K. 2003, Coupling the cell cycle to cell growth, *EMBO Rep.*, **4**, 757–60.
17. Wang, J.D. and Levin, P.A. 2009, Metabolism, cell growth and the bacterial cell cycle, *Nat. Rev. Microbiol.*, **7**, 822–7.
18. Barańska, S., Glinkowska, M. and Herman-Antosiewicz, A. 2013, Replicating DNA by cell factories: roles of central carbon metabolism and transcription in the control of DNA replication in microbes, and implications for understanding this process in human cells, *Microb. Cell Fact.*, **12**, 55.
19. Lark, K.G., Repko, T. and hoffman, E.J. 1963, The effect of amino acid deprivation on subsequent deoxyribonucleic acid replication, *Biochimica Et Biophysica Acta (BBA) - General Subjects*, **76**, 9–24.
20. Copeland, J.C. 1971, Regulation of chromosome replication in *Bacillus subtilis*: marker frequency analysis after amino acid starvation, *Science*, **172**, 159–61.
21. Levine, A., Vannier, F., Dehbi, M., Henckes, G. and Séror, S.J. 1991, The stringent response blocks DNA replication outside the *ori* region in *Bacillus subtilis* and at the origin in *Escherichia coli*, *J. Mol. Biol.*, **219**, 605–13.
22. DeNapoli, J., Tehranchi, A.K. and Wang, J.D. 2013, Dose-dependent reduction of replication elongation rate by (p)ppGpp in *Escherichia coli* and *Bacillus subtilis*, *Mol. Microbiol.*, **88**, 93–104.
23. Wang, J.D., Sanders, G.M. and Grossman, A.D. 2007, Nutritional control of elongation of DNA replication by (p)ppGpp, *Cell*, **128**, 865–75.
24. Maciag, M., Kochanowska, M., Lyzeń, R., Wegrzyn, G. and Szalewska-Pałasz, A. 2010, ppGpp inhibits the activity of *Escherichia coli* DnaG primase, *Plasmid*, **63**, 61–7.
25. Hernandez, J.V. and Bremer, H. 1993, Characterization of RNA and DNA synthesis in *Escherichia coli* strains devoid of ppGpp, *J. Biol. Chem.*, **268**, 10851–62.
26. Monahan, L.G., Hajduk, I.V., Blaber, S.P., Charles, I.G. and Harry, E.J. 2014, Coordinating bacterial cell division with nutrient availability: a role for glycolysis, *Mbio.*, **5**, e00935–14.
27. Vadia, S. and Levin, P.A. 2015, Growth rate and cell size: a re-examination of the growth law, *Curr. Opin. Microbiol.*, **24**, 96–103.
28. Westfall, C.S. and Levin, P.A. 2018, Comprehensive analysis of central carbon metabolism illuminates connections between nutrient availability, growth rate, and cell morphology in *Escherichia coli*, *PLoS Genet.*, **14**, e1007205–25.
29. Jannière, L., Canceill, D., Suski, C., et al. 2007, Genetic evidence for a link between glycolysis and DNA replication, *PLoS One.*, **2**, e447.
30. Rannou, O., Le Chatelier, E. and Larson, M.A. 2013, Functional interplay of DnaE polymerase, DnaG primase and DnaC helicase within a ternary complex, and primase to polymerase hand-off during lagging strand DNA replication in *Bacillus subtilis*, *Nucleic Acids Res.*, **41**, 5303–20.
31. Paschalis, V., Le Chatelier, E., Green, M., Képès, F., Soultanas, P. and Jannière, L. 2017, Interactions of the *Bacillus subtilis* DnaE polymerase with replisomal proteins modulate its activity and fidelity, *Open Biol.*, **7**, 170146.
32. Maciąg, M., Nowicki, D., Jannière, L., Szalewska-Pałasz, A. and Wegrzyn, G. 2011, Genetic response to metabolic fluctuations: correlation between central carbon metabolism and DNA replication in *Escherichia coli*, *Microb. Cell Fact.*, **10**, 19.
33. Maciąg-Dorszyńska, M., Ignatowska, M., Jannière, L., Węgrzyn, G. and Szalewska-Pałasz, A. 2012, Mutations in central carbon metabolism genes suppress defects in nucleoid position and cell division of replication mutants in *Escherichia coli*, *Gene*, **503**, 31–5.
34. Tymecka-Mulik, J., Boss, L., Maciąg-Dorszyńska, M., et al. 2017, Suppression of the *Escherichia coli dnaA46* mutation by changes in the activities of the pyruvate-acetate node links DNA replication regulation to central carbon metabolism, *PLoS One*, **12**, e0176050.
35. Chen, Y. and Tye, B.-K. 1995, The yeast Mcm1 protein is regulated posttranscriptionally by the flux of glycolysis, *Mol. Cell. Biol.*, **15**, 4631–9.
36. Chang, V.K., Fitch, M.J., Donato, J.J., Christensen, T.W., Merchant, A.M. and Tye, B.K. 2003, Mcm1 binds replication origins, *J. Biol. Chem.*, **278**, 6093–100.
37. Kaplan, Y. and Kupiec, M. 2007, A role for the yeast cell cycle/splicing factor Cdc40 in the G1/S transition, *Curr. Genet.*, **51**, 123–40.
38. He, H., Lee, M.C., Zheng, L.L., Zheng, L. and Luo, Y. 2013, Integration of the metabolic/redox state, histone gene switching, DNA replication and S-phase progression by moonlighting metabolic enzymes, *Biosci. Rep.*, **33**, e00018.
39. Konieczna, A., Szczepańska, A., Sawiuk, K., Wegrzyn, G. and Łyżeń, R. 2015, Effects of partial silencing of genes coding for enzymes involved in

glycolysis and tricarboxylic acid cycle on the enterance of human fibroblasts to the S phase, *BMC Cell Biol*., **16**, 16.
40. Fornalewicz, K., Wieczorek, A., Węgrzyn, G. and Łyżeń, R. 2017, Silencing of the pentose phosphate pathway genes influences DNA replication in human fibroblasts, *Gene*, **635**, 33–8.
41. Gangwe Nana, G.Y., Ripoll, C., Cabin-Flaman, A., et al. 2018, Division-based, growth rate diversity in bacterial, *Front. Microbiol*., **9**, 849.
42. Norris, V., Képès, F., Amar, P., Koch, I. and Jannière, L. 2017, Hypothesis: local variations in the speed of individual DNA replication forks determine the phenotype of daughter cells, *Med. Res. Arch*., **5**, 1598.
43. Sezonov, G., Joseleau-Petit, D. and D'Ari, R. 2007, *Escherichia coli* physiology in Luria-Bertani broth, *J. Bacteriol*., **189**, 8746–9.
44. Vagner, V., Dervyn, E. and Ehrlich, D.S. 1998, A vector for systematic gene inactivation in *Bacillus subtilis*, *Microbiology*, **144**, 3097–104.
45. Britton, R.A., Eichenberger, P., Gonzalez-Pastor, J.E., Fawcett, P., Monson, R., Losick, R. and Grossman, A.D. 2002, Genome-wide analysis of the stationary-phase sigma factor (Sigma-H) regulon of *Bacillus subtilis*, *J. Bacteriol*., **184**, 4881–90.
46. Svitil, A.L., Cashel, M. and Zyskind, J.W. 1993, Guanosine tetraphosphate inhibits protein synthesis in vivo: a possible protective mechanism for starvation stress in *Echerichia coli*, *J. Biol. Chem*., **268**, 2307–11.
47. Guérout-Fleury, A.-M., Frandsen, N. and Stragier, P. 1996, Plasmids for ectopic integration in *Bacillus subtilis*, *Gene*, **180**, 57–61.
48. Titok, M.A., Chapuis, J., Selezneva, Y.V., Lagodich, A.V., Prokulevich, V.A., Ehrlich, S.D. and Jannière, L. 2003, *Bacillus subtilis* soil isolates: plasmid replicon analysis and construction of a new theta-replicating vector, *Plasmid*, **49**, 53–62.
49. Uicker, W.C., Schaefer, L. and Britton, R.A. 2006, The essential GTPase RbgA (YlqF) is required for 50S ribosome assembly in *Bacillus subtilis*, *Mol. Microbiol*., **59**, 528–40.
50. Magill, N.G. and Setlow, P. 1992, Properties of purified sporlets produced by spoII mutants of Bacillus subtilis, *J. Bacteriol*., **174**, 8148–51.
51. Stokke, C., Flåtten, I. and Skarstad, K. 2012, An easy-to-use simulation program demonstrates variations in bacterial cell cycle parameters depending on medium and temperature, *PLoS ONE*, **7**, e30981.
52. Zheng, H., Ho, P.-Y., Jiang, M., et al. 2016, Interrogating the *Escherichia coli* cell cycle by cell dimension perturbations, *Proc. Natl. Acad. Sci. USA*., **113**, 15000–5.
53. Séror, S.J., Casarégola, S., Vannier, F., Zouari, N., Dahl, M. and Boye, E. 1994, A mutant cysteinyl-tRNA synthetase affecting timing of chromosomal replication initiation in *B. subtilis* and conferring resistance to a protein kinase C inhibitor, *Embo J*, **13**, 2472–80.,
54. Hill, N.S., Kadoya, R., Chattoraj, D.K. and Levin, P. A. 2012, Cell size and the initiation of DNA replication in bacteria, *PLoS Genet*., **8**, e1002549.
55. Vinella, D., Albrecht, C., Cashel, M. and D'Ari, R. 2005, Detection of (p)ppGpp accumulation patterns in *Escherichia coli* mutants, *Methods Mol Genet*, **56**, 958–6.,
56. Koga, K., Ikegami, A., Nakasone, K., et al. 2006, Construction of *Bacillus subtilis* strains carrying the transcriptional *bgaB* fusion with the promoter region of each *rrn* operon and their differential transcription during spore development, *J. Gen. Appl. Microbiol*., **52**, 119–24.
57. Westers, H., Dorenbos, R. and Van Dijl, J.M. 2003, Genome engineering reveals large dispensable regions in *Bacillus subtilis*, *Molecular Biology and Evolution*, **20**, 2076–90.
58. Sueoka, N. and Yoshikawa, H. 1965, The chromosome of *Bacillus subtilis*: i. Theory of marker frequency analysis. *Genetics*, **52**, 747–57.
59. Schreiber, G., Metzger, S., Aizenman, E., Roza, S., Cashel, M. and Glaser, G. 1991, Overexpression of the *relA* gene in *Escherichia coli*, *J. Biol. Chem*, **266**, 3760–7.
60. Potrykus, K. and Cashel, M. 2008, (p)ppGpp: still magical? *Annu. Rev. Microbiol*., **62**, 35–51.
61. Tanaka, T. and Ogura, M. 1998, A novel *Bacillus natto* plasmid pLS32 capable of replication in *Bacillus subtilis*, *FEBS Lett*., **422**, 243–6.
62. Tanaka, T., Ishida, H. and Maehara, T. 2005, Characterization of the replication region of plasmid pLS32 from the Natto strain of *Bacillus subtilis*, *J. Bacteriol*., **187**, 4315–26.
63. Hassan, A.K.M., Moriya, S., Ogura, M., Tanaka, T., Kawamura, F. and Ogasawara, N. 1997, Suppression of initiation defects of chromosome replication in *Bacillus subtilis dnaA* and *oriC*-deleted mutants by integration of a plasmid replicon into the chromosomes, *J. Bacteriol*., **179**, 2494–502.
64. Moriya, S., Hassan, A.K.M., Kadoya, R. and Ogasawara, N. 1997, Mechanism of anucleate cell production in the *oriC*-deleted mutants of *Bacillus subtilis*, *DNA Res*., **4**, 115–26.
65. Bird, L.E., Pan, H., Soultanas, P. and Wigley, D.B. 2000, Mapping protein–protein interactions within a stable complex of DNA primase and DnaB helicase from *Bacillus stearothermophilus*, *Biochemistry*, **39**, 171–82.
66. Velten, M., McGovern, S., Marsin, S., Ehrlich, S.D., Noirot, P. and Polard, P. 2003, A two-protein strategy for the functional loading of a cellular replicative DNA helicase, *Mol. Cell*., **11**, 1009–20.
67. Liu, B., Eliason, W.K. and Steitz, T.A. 2013, Structure of a helicase–helicase loader complex reveals insights into the mechanism of bacterial primosome assembly, *Nat. Commun*., **4**, 2495.
68. Dervyn, E., Suski, C., Daniel, R., et al. 2001, Two essential DNA polymerases at the bacterial replication fork, *Science*, **294**, 1716–9.
69. Sanders, G.M., Dallmann, H.G. and McHenry, C.S. 2010, Reconstitution of the *B. subtilis* replisome with 13 proteins including two distinct replicases, *Mol. Cell*., **37**, 273–81.
70. Briggs, G.S., Smits, W.K. and Soultanas, P. 2012, Chromosomal replication initiation machinery of low-G+C-content firmicutes, *J. Bact*., **194**, 5162–70.
71. Lee, J.-B., Hite, R.K., Hamdan, S.M., Xie, S.X., Richardson, C.C. and van Oijen, A.M. 2006, DNA primase acts as a molecular break in DNA replication, *Nature*, **439**, 621–4.
72. Tanner, N.A., Hamdan, S.M., Jergic, S., Loscha, K.V., Schaeffer, P.M., Dixon, N.E. and van Oijen, A.M. 2008, Single-molecule studies of fork dynamics in *Escherichia co*li DNA replication, *Nat. Struct. Mol. Biol*., **15**, 170–6.
73. Yao, N.Y., Georgescu, R.E., Finkelstein, J. and O'Donnell, M.E. 2009, Single-molecule analysis reveals that the lagging strand increases replisome processivity but slows replication fork progression, *P. Natl. Aca. Sci. USA*, **106**, 13236–41.
74. Georgescu, R.E., Yao, N., Indiani, C., Yurieva, O. and O'Donnell, M.E. 2014, Replisome mechanics: lagging strand events that influence speed and processivity, *Nucleic Acids Res*., **42**, 6497–510.
75. Stano, N.M., Jeong, Y.-J., Donmez, I., Tummalapalli, P., Levin, M.K. and Patel, S.S. 2005, DNA synthesis by a polymerase provides the driving force to accelerate DNA unwinding by a helicase, *Nature*, **435**, 370–3.
76. Indiani, C., Langston, L.D., Yurieva, O., Goodman, M.F. and O'Donnell, M.E. 2009, Translesion DNA polymerases remodel the replisome and alter the speed of the replicative helicase, *Proc. Natl. Acad. Sci. USA*., **106**, 6031–8.
77. Graham, J.E., Marians, K.J. and Kowalczykowski, S.C. 2017, Independent and stochastic action of DNA polymerases in the replisome, *Cell*, **169**, 1201–17.
78. Kelly, T.J. and Brown, G.W. 2000, Regulation of chromosome replication, *Annu. Rev. Biochem*., **69**, 829–80.
79. Wei, L. and Zhao, X. 2016, Role of posttranslational modifications in replication initiation In: Kaplan, D. D., (ed.), *The Initiation of DNA Replication in Eukaryotes*. Springer International Publishing, pp. 371–92.
80. van Noort, V., Seebacher, J., Bader, S., et al. 2012, Cross-talk between phosphorylation and lysine acetylation in a genome-reduced bacterium, *Mol. Syst. Biol*., **8**, 571.
81. Hentchel, K.L. and Escalante-Semerena, J.C. 2015, Acylation of biomolecules in prokaryotes: a widespread strategy for the control of biological function and metabolic stress, *Microbiol. Mol. Biol. Rev*., **79**, 321–46.

82. Garcia-Garcia, T., Poncet, S., Derouiche, A., Shi, L., Mijakovic, I. and Noirot-Gros, M.-F. 2016, Role of protein phosphorylation in the regulation of cell cycle and DNA-related processes in bacteria, *Front. Microbiol.*, **7**, 184.
83. Shi, L., Pigeonneau, N., Ventroux, M., et al. 2014, Protein-tyrosine phosphorylation interaction network in *Bacillus subtilis* reveals new substrates, kinase activators and kinase cross-talk, *Front. Microbiol.*, **5**, 538.
84. Zhang, Q., Zhou, A., Li, S., et al. 2016, Reversible lysine acetylation is involved in DNA replication initiation by regulating activities of initiator DnaA in *Escherichia coli*, *Sci. Rep.*, **6**, 30837.
85. Mijakovic, I., Petranovic, D., Macek, B., et al. 2006, Bacterial single-stranded DNA-binding proteins are phosphorylated on tyrosine, *Nucleic Acids Res.*, **34**, 1588–96.
86. Petranovic, D., Michelsen, O., Zahradka, K., et al. 2007, *Bacillus subtilis* strain deficient for the protein-tyrosine kinase PtkA exhibits impaired DNA replication, *Mol. Microbiol.*, **63**, 1797–805.
87. Cai, L., Sutter, B.M., Li, B. and Tu, B.P. 2011, Acetyl-CoA induces cell growth and proliferation by promoting the acetylation of histones at growth genes, *Mol. Cell.*, **42**, 426–37.
88. Ladurner, A.G. 2006, Rheostat control of gene expression by metabolites, *Mol. Cell.*, **24**, 1–11.
89. Chubukov, V., Gerosa, L., Kochanowski, K. and Sauer, U. 2014, Coordination of microbial metabolism, *Nat. Rev. Microbiol.*, **12**, 327–40.
90. Grangeasse, C., Nessler, S. and Mijakovic, I. 2012, Bacterial tyrosine kinases: evolution, biological function and structural insights, *Philos. Trans. R Soc. Lond, B, Biol. Sci.*, **367**, 2640–55.
91. Guan, K.-L. and Xiong, Y. 2011, Regulation of intermediary metabolism by protein acetylation, *Trends Biochem. Sci.*, **36**, 108–16.
92. Weinert, B.T., Iesmantavicius, V., Wagner, S.A., et al. 2013, Acetyl-phosphate is a critical determinant of lysine acetylation in *E. coli*, *Mol. Cell.*, **51**, 265–72.
93. Wolfe, A.J. 2010, Physiologically relevant small phosphodonors link metabolism to signal transduction, *Curr. Opin. Microbiol.*, **13**, 204–9.
94. Kim, J.-W. and Dang, C.V. 2005, Multifaceted roles of glycolytic enzymes, *Trends Biochem. Sci.*, **30**, 142–50.
95. Sirover, M.A. 2011, On the functional diversity of glyceraldehyde-3-phosphate dehydrogenase: biochemical mechanisms and regulatory control, *BBA - General Subjects*, **1810**, 741–51.
96. Norris, V., Amar, P., Legent, G., Ripoll, C., Thellier, M. and Ovadi, J. 2013, Sensor potency of the moonlighting enzyme-decorated cytoskeleton: the cytoskeleton as a metabolic sensor, *BMC Biochem.*, **14**, 3.
97. Boukouris, A.E., Zervopoulos, S.D. and Michelakis, E.D. 2016, Metabolic enzymes moonlighting in the nucleus: metabolic regulation of gene transcription, *Trends Biochem. Sci.*, **41**, 712–30.
98. Michel, B., Florès, M.-J., Viguera, E., Grompone, G., Seigneur, M. and Bidnenko, V. 2001, Rescue of arrested replication forks by homologous recombination, *Proc. Natl. Acad. Sci. USA.*, **98**, 8181–8.
99. Rodgers, K. and McVey, M. 2016, Error-Prone repair of DNA double-strand breaks, *J. Cell. Physiol.*, **231**, 15–24.
100. Arias, E.E. and Walter, J.C. 2007, Strength in numbers: preventing rereplication via multiple mechanisms in eukaryotic cells, *Genes Dev.*, **21**, 497–518.
101. Mehta, A. and Haber, J.E. 2014, Sources of DNA double-strand breaks and models of recombinational DNA repair, *Cold Spring Harb. Perspect. Biol.*, **6**, a016428.
102. Maciąg, M., Nowicki, D., Szalewska-Pałasz, A. and Wegrzyn, G. 2012, Central carbon metabolism influences fidelity of DNA replication in *Escherichia coli*, *Mutat. Res.*, **731**, 99–106.
103. Shi, I.Y., Stansbury, J. and Kuzminov, A. 2005, A Defect in the acetyl coenzyme A acetate pathway poisons recombinational repair-deficient mutants of *Escherichia coli*, *J. Bact.*, **187**, 1266–75.
104. Chen, Z., Odstrcil, E.A., Tu, B.P. and McKnight, S.L. 2007, Restriction of DNA replication to the reductive phase of the metabolic cycle protects genome integrity, *Science*, **316**, 1916–9.
105. Gatenby, R.A. and Gillies, R.J. 2004, Why do cancers have high aerobic glycolysis?, *Nat. Rev. Cancer*, **4**, 891–9.
106. Loeb, L.A., Loeb, K.R. and Anderson, J.P. 2003, Multiple mutations and cancer, *Proc. Natl. Acad. Sci. USA.*, **100**, 776–81.
107. Tubbs, A. and Nussenzweig, A. 2017, Endogenous DNA damage as a source of genomic instability in cancer, *Cell*, **168**, 644–56.